

# Mapping of Optical Parameters of Aerosols over Land using Multi-Spectral IRS-P4 OCM Sensor Data

Rajshree Rege<sup>#</sup>, M. B. Potdar<sup>#</sup>, P. C. S. Devara<sup>@</sup> and B. P. Agrawal<sup>&</sup>

<sup>#</sup>Space Applications Centre, Ahmedabad 380 015, mbpotdar@sac.isro.gov.in

<sup>@</sup>Indian Institute of Tropical Meteorology, Pune 410 008

<sup>&</sup>Dept. of Physics, Gujarat University, Ahmedabad 380 009

Rajshree Rege, Commission WG-IV/10, No. WG-410-211

**Key Words:** Atmospheric aerosol, parametric aerosol models, Spatial Mapping, OCM land Data, Seasonal Variation

## Abstract:

A methodology has been developed for modeling and mapping various aerosol parameters using the IRS-P4 Ocean Color Monitoring [OCM] multi-spectral data having wide swath of 1420 km and high (360 m) spatial resolution and high (2 days ) temporal coverage. OCM images in 8 spectral bands at radiometric resolution of 12 bits. In the present work, a methodology to retrieve aerosol properties from the satellite data is reported. A primary analysis for studying the change in aerosol types and their distribution in time is reported. More than 60 dates of OCM data covering Dec to May period of 2001, 2002 and 2004 along with the sun-photometric data at Indian Institute of Tropical Meteorology [IITM] Pune, India and Space Applications Centre [SAC], Ahmedabad, India for mapping Aerosol Optical Thickness [AOT] at 412, 443, 500, and 670 nm using satellite measured radiances from Thick Vegetation Targets [TVT]. Due to strong chlorophyll absorption in blue and red spectral regions, the TVT acts as potential dark background targets in helping to delineate the aerosol parameters from satellite measured radiances. The results show that the OCM measured radiances over TVTs are able to detect the changing nature of the aerosol and/or their radiative properties. Three distinct parametric models to retrieve AOT at each of three wavelengths 412 nm, and 443 nm corresponding to 3 bimonthly periods and two models at 500 nm for two tri-monthly periods are found to exist, which describe the changing radiative properties from Dec. to May. The model performances have been tested for the IITM and SAC sites and have been validated using independent data sets collected at and within 100 km of IITM, Pune and SAC, Ahmedabad. Methodology for spatial mapping of aerosol characteristics viz. AOT, Angstrom exponent and turbidity coefficient are developed for an area of 180x180 km of interest in atmospheric correction of high spatial resolution remote sensing data and Global Atmospheric General Circulation modeling. A preliminary analysis using Sun Photometer derived Angstrom Exponent [AE] is carried out in order to characterize the systematic change exhibited by parametric aerosol models.

## Introduction

Atmospheric aerosol is a system consisting of fine particles, solid or liquid, suspended in the atmosphere. This suspended particulate matter along with the atmospheric gases alters the net amount of radiation available at the earth's surface and at the Top of the Atmosphere (TOA). In order to study the effect of intervening atmosphere on the earth's radiation budget, the optical characteristics of the atmosphere are extensively used. Molecular scattering and ozone absorption, considered as invariant effects, are accounted for satisfactorily, but it is difficult to estimate aerosol's effect on the radiation traversing through the earth's atmosphere due to their variation in space and time. The cause of high spatial and temporal variability shown by aerosol is the variety of sources and sinks of aerosol particles and meteorological conditions. Depending up on the seasonal meteorological conditions aerosols are transported from their sources to the distant places in all directions and their vertical distribution in the atmosphere also keeps changing in time. Elevated aerosol layers can be picked up by strong winds and can be transported from one continent to another. Aerosol properties are modified during the transport by dry or wet deposition, in cloud processes and by atmospheric chemical reactions [1]. The aerosol investigation therefore requires the identification of source regions, their strength and aerosol type, the determination of variable turbidity of the region and the

regional meteorological conditions viz. wind profile, temperature and humidity [5]. A quantitative assessment of the aerosol effects on the climate requires a better knowledge of their global distribution and characteristics [2]. To accurately study aerosol distribution, continuous observation from satellites, networks of ground based instruments and dedicated field experiments are required. Satellites with their capability for large area coverage and short-term repetivity are the most ideal means for acquiring global information on aerosol. Satellite based remote sensing of aerosol has started with the detection of a thick aerosol layer from large scale dust storm or forest fire events, which can be easily detected by an enhanced reflectance in a visible channel. With the advancement in technology satellites systems are now available with the ability to observe and study the spatial distribution of many aerosol parameters on a larger scale. With single channel sensors it was possible to map Aerosol Optical Thickness (AOT) only, now with the use of multi channel, multi-view angle and polarization sensitive sensors it is possible to map a number of aerosol parameters like aerosol size distribution, single scattering albedo, refractive index etc. In the present work a methodology to retrieve aerosol properties e.g. AOT, angstrom exponent and turbidity coefficient using TOA radiance from in 412, 443, 500 and 670 nm bands of the IRS-P4, OCM data is reported. Also, a

primary analysis for studying the change in aerosol types and  
**Study Area and Data Used**

For the present analysis, IRS-P4 Ocean Color Monitoring (OCM) land data and synchronously collected Ground based sun photometric data at IITM, Pune (Latitude: 18° 32', Longitude: 73° 48') and SAC Ahmedabad (Latitude: 23°20', Longitude: 72°31') are used to model and map the AOT at 412, 443, 500 and 670 nm. Overall 60 date data of the years 2001 and 2002 at IITM Pune and of the years 2003 and 2004 at SAC,

their distribution in time is reported.

Ahmedabad were selected on the basis of atmospheric stability and sky conditions for the model development (Potdar et al. 2004). The OCM sensor specifications are given in table.1. For validation the sun photometer data collected at Daund, situated at 84 km east of IITM and corresponding OCM data are used. Microtops-II sun photometer (Manufactured by Solar Light Co., USA), used to ground truth, accounts for Rayleigh scattering and O<sub>3</sub> absorption and gives the direct value of AOT at six wavelengths viz 340, 440, 500, 670 870 and 1020 nm.

**Table 1: Specifications of IRS-P4 OCM Sensor**

Date of Launch	26 May 1999.	
IGFOV	360 m Across Track 236 m Along Track (Finally sampled to 360 m in both directions)	
Swath	1420 km	
Repetivity	2 Days	
Altitude	720 km	
Equatorial Crossing Time	7 hr 21 m GMT	
No. of Spectral Band	8	
Spectral range (Band centre)	1) 402 – 422 nm (412)	5) 545 – 565 nm (555)
	2) 433 – 453 nm (443)	6) 660 – 680 nm (670)
	3) 480 – 500 nm (490)	7) 745 – 785 nm (765)
	4) 500 – 520 nm (510)	8) 845 – 885 nm (865)
Quantization level	12 bits (Finally scaled to 16 bit)	
Saturation Radiance (W/m <sup>2</sup> .nm.sr)	1) 49.10	5) 18.34
	2) 28.80	6) 14.10
	3) 23.54	7) 6.57
	4) 22.05	8) 10.96

**Methodology**

The method followed to retrieve aerosol properties from OCM, the space born sensor is described under the following headings:

1. Principle
2. Identification of thick vegetation pixels.
3. Parametric Model development and validation.
4. Generation of AOT maps.
5. Mapping of size distribution parameters.

1. The retrieval of Aerosol Optical Thickness (AOT) has been a starting point of several atmospheric investigations. AOT quantifies the attenuation of sunlight by the atmospheric particulate matter and thus serves as a measure of aerosol column concentration. The present methodology, developed to retrieve Aerosol optical thickness over land from TOA radiance measured by OCM sensor, is based on the dark (low reflectance) target approach. Due to the strong chlorophyll absorption in both blue and red bands and their absorption profile wing effect in green band, vegetation acts as low reflectance target in the visible region. In a broader view, the TOA radiance comes from two contributions, one is the surface reflection and the other is atmospheric radiative transfer processes. In case of the thick vegetation pixels, having reflectance of nearly  $2 \pm 1$  to  $3 \pm 1$  % in blue and red wavelength bands respectively and about 5 to 8 ( $\pm 2$  %) in green band, the

TOA radiance consists mostly of the backscattered radiance by the atmosphere. Further atmospheric signal is a result of Rayleigh scattering by air molecules, which is nearly constant in time and the Mie scattering by aerosol particles, which is highly variable in both time and space. Hence for a constant low reflectance surface any change observed in the measured TOA corresponds to the change in aerosol concentration, altitude profile and/or their microphysical properties.

2. The thick vegetation targets are identified by the Normalized Difference Vegetation Index (NDVI) derived from the NIR and Red band radiance data of the OCM. NDVI is defined as follows:

$$NDVI = (R_{NIR} - R_{RED}) / (R_{NIR} + R_{RED}),$$

Where R<sub>NIR</sub>, R<sub>RED</sub> are radiances in RED (670 nm) and NIR (870 nm) bands. For vegetation targets, it ranges from 0.05 to 1.

The NDVI images are generated for the area centered at IITM, Pune and SAC, Ahmedabad and TVTs are picked up based on NDVI > 0.5. Because of the effect of intervening atmosphere the NDVI computed from the TOA radiances would always be lower than that computed at the surface. The choice of NDVI>0.5 derived from the

OCM radiances would therefore serve as a good criterion for the identification of a thick vegetation pixel at the earth's surface, as the surface NDVIs would be still greater than 0.5. It is found that good number of TVTs could be found with OCM data at 360 m spatial resolution. The TVTs could be highly ubiquitous with higher spatial resolution data.

3. For model development purpose regular Sun photometric measurements are carried out at IITM, Pune and SAC, Ahmedabad. Plot of the radiance in 412, 443, 500 and 670 nm bands vs. NDVI is generated from the data in the grid of size 18 km X 18 km centered at sun photometric measurement site (viz. IITM and SAC). It is found that the radiances in three channels decrease with increasing NDVI and ultimately reach asymptotic values at large NDVI, (typically at NDVI > 0.5). This decrease in NDVI is expected for 670 nm as it is used in NDVI computation. This pattern is observed even for 412, 443 and 500 nm bands, which do not go into computation of NDVI. Here we use NDVI as a measure of thickness or chlorophyll content of vegetation target. We do not use NDVI per se in any quantitative evaluation or in further computation in AOT retrieval. By fitting a power law in NDVI, the limiting value of the TOA radiances are computed. The derived limiting value of radiance is used to model AOT in respective bands. The asymptotic radiance values are corrected for the solar zenith angle, to account for illumination effects or normalize for vertical solar irradiance and for sensor view angle. Corrected radiances then, are related to the AOT measured by sun photometer [fig.1] near synchronous to pass of the IRS-P4 satellite. Model equations to retrieve AOT from the TOA radiance are developed.

4. Aerosol model equation is fitted for each of the three periods for 412 and 443 nm wavelength bands (Table 2). At 500 nm band however the data can be grouped into two tri-monthly periods; one for Dec-Jan-Feb and other for Mar-Apr-May. Here it should be mentioned that no sharp boundary exists between any two groups of the data set at any wavelength. Since the aerosol microphysical characteristics vary continuously through the course of time from Dec. to May, in these regions under study, the grouping in two month periods are found to be adequate to represent the continuous changing aerosols given the errors in the AOT measurements and TVT radiances from satellite data.

At 670 nm whole data can be grouped into three groups and we get three models corresponding to each group. However, at this wavelength, the grouping does not follow the bimonthly time periods. This is due to significant contribution from the second coarse mode component of aerosols due to diurnal human activities which is highly variable from day to day. The 500 nm data points act as anchor points below and above which the AOT vary significantly and variations are in general opposite direction. In general, high AOTs at < 500 nm are associated with low AOTs at > 500 nm; as aerosols follow the Junge or modified Junge size distribution model [14].

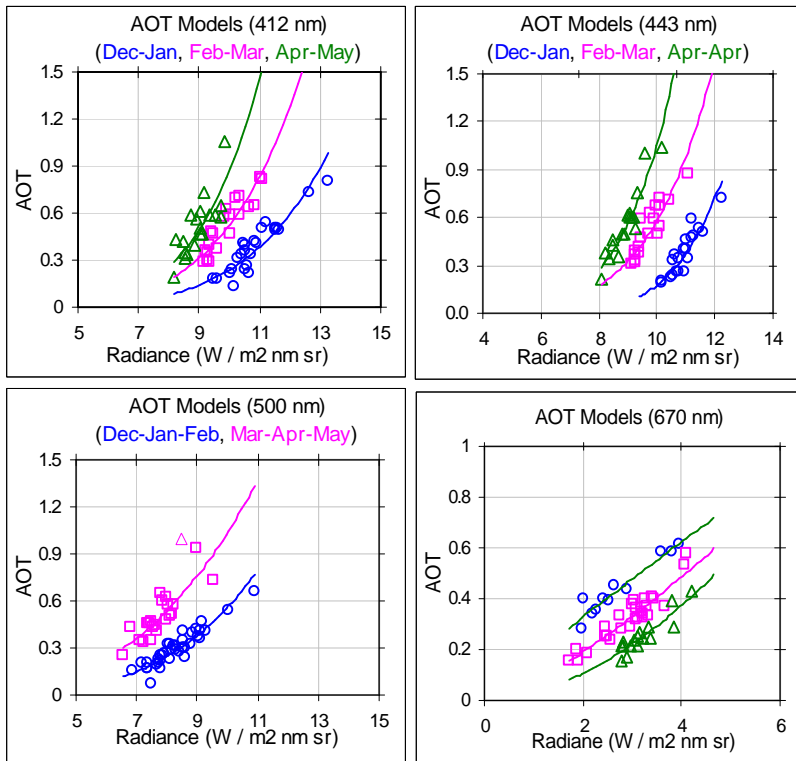


**Fig.1: AOT Modeling using OCM Land Data over Thick Vegetation Targets. Different colors represent different time periods from Dec. to May. At 412 and 443 nm, blue, pink and green points correspond to Dec.-Jan, Feb-Mar and Apr- May periods, respectively. For 500 nm, Blue and pink represents Dec-Jan-Feb and Mar-Apr-May periods, respectively. At 670 nm three groups are seen, but unlike other wavelengths, do not correspond to any specific time periods.**

**Table2. Time period-wise parametric models. Here y stands for AOT and x for corrected TOA radiance.**

S. N.	Months	l in nm	Model Equation	R <sup>2</sup>
1	Dec-Jan	412	$y = 3.1860E-06x^{5.0098}$	0.74
2	Feb-Mar	412	$y = 6.8321E-06x^{4.8833}$	0.80
3	Apr-May	412	$y = 3.5060E-06x^{5.3948}$	0.64
4	Dec-Jan	443	$y = 4.4128E-06x^{4.9482}$	0.80
5	Feb-Mar	443	$y = 1.8862E-06x^{5.4882}$	0.79
6	Apr-May	443	$y = 8.8337E-07x^{6.0787}$	0.85
7	Dec-Jan-Feb	500	$y = 0.0001x^{3.7219}$	0.74
8	Mar-Apr-May	500	$y = 0.0012x^{2.9373}$	0.71
9	Group1	675	$y = 0.1732x^{0.9247}$	0.89
10	Group2	675	$y = 0.075x^{1.3488}$	0.90
11	Group3	675	$y = 0.0303x^{1.8123}$	0.77

- The AOT maps are generated over 180x180 km<sup>2</sup> area centred at sun-photometric measurements sites of IITM at Pune and SAC at Ahmedabad. The area of this dimensions normally cover a typical remote sensing scene of spatial resolution from 20 to 100 m and also 1 to 1.5 degree latitude-longitude grid, over which the average of various meteorological parameters are used in Atmospheric Global Circulation Modes (A-GCMs). The average aerosol radiative forcing over such an area can be a direct input to AGCMs. The area is divided into 100 grids of each 18 kmx18 km size. For each grid, the asymptotic values of the radiances in 412, 443, 500 and 670 nm with increasing NDVI are determined. The asymptotic radiances for each grid are then corrected for the solar zenith angle as well as sensor view angle. From the corrected radiances, the AOTs are computed using model equations for the respective time periods (shown in Fig. 2 and table 2). The estimated AOTs are assigned to the center of the respective grids, and then a spatial contour map of AOT is generated by interpolating grid center values following method of Kriging with linear variogram.
- Angstrom exponent ( $\alpha$ ) which is defined as the slope of the spectral dependence of AOT [1] is related to the Junge size distribution parameter ( $\nu$ ), as  $\nu = \alpha + 2$ . Curcio (1961) [14] used the wavelength dependence of the extinction coefficient in the visible and NIR and showed that the majority of aerosol size distributions could best be represented by a two component size distribution or modified Junge size distribution consisting of a Junge size distribution plus a small component of larger size particles. The validity of the modified Junge size distribution for the Pune region is also reported in a previous study using reservoir as dark targets (Potdar et al. 2004) [7]. The pixel-wise interpolated AOTs at four wavelengths are used to derive and map size distribution parameters namely angstrom exponent and turbidity coefficient. Measured spectral AOT curves are used to derive the values of above mentioned size distribution parameters. Size distribution parameters derived from the measured AOT values are then compared with the mapped ones to check the reliability of the maps. The model performance was checked by comparing the model derived AOTs with the measured ones for the IITM and SAC sites. It is found that the OCM retrieved AOTs compare very

with the measured AOTs. Also, most importantly, the models are validated using an independent data set at Daund, which is situated nearly 85 km east of Pune. The modeled AOTs at 412, 443, 500 and 670 nm are compared with the measured AOTs in fig. 2. Except the AOTs at 412 nm, the agreement is quite good at all the other wavelengths. At 412 nm, the OCM data retrieved AOT are higher by about 16%. The angstrom exponent and turbidity coefficients are also found to be in good agreement with measured ones at this place of measurement.

## Results and Discussion

The TOA radiance is composed of the path radiance and the transmitted radiance from the surface irradiated by the global irradiance. As discussed above the Rayleigh part can be assumed to be constant. Any change observed in the TOA radiance can be attributed to the change in aerosol type, their altitude and size distributions and/or their concentration, given that the surface reflectance is not changing in time. In the present work parametric models have been derived to retrieve AOT at 412 nm, 443 nm, 500 nm and 670 nm wavelength bands using IRS-P4 OCM measured TOA radiance data over thick vegetation target and the sun photometer data set collected near-synchronous to the IRS-P4 pass. It is observed that from Dec. to May there is an increase in outgoing TOA radiance associated with the nearly same AOT values, resulting in different parametric models for successive bimonthly period. This indicates some gradual change in aerosol properties from Dec. to May, which is reflected in the different models. In retrieval of AOT from TOA radiance at any of the wavelengths the aerosol layer height and Single Scattering Albedo (SSA) play dominant roles in determining TOA out going radiance from a dark target [9]. Aerosol layer height is determined by the structure of inversion layer associated with the seasonal meteorological conditions while SSA, a measure of absorption by aerosol, depends on the aerosol sources, relative humidity and meteorological conditions. SSA and its spectral behavior depend on the particle's chemical composition. For example, in case of desert dust, composed of mostly mineral compounds, SSA increases with wavelength while for biomass burning aerosol it decreases with wavelength [12]. Change in temperature and humidity would affect the overall composition of aerosol. In summers, increase in temperature would result in decreased soil moisture, as consequence dust content would increase in the atmosphere. Also increased temperature would reduce the amount of water vapor in the atmosphere, due to this smaller sized bare pollutant particles would be produced, which were otherwise coated with water. In this way change in temperature and humidity would alter the aerosol size distribution and would change the aerosol composition. A study on seasonal variation in AOT for three urban sites in India by Jethva et al. [7], based on the analysis of MODIS AOT product and Fine Mode Aerosol Fraction [FMAF] product, low values of FMAF or abundance of coarse mode dust particles was reported in summers. Similar trend is also found for Ahmedabad and Pune.

Difference observed in the TOA radiance measured by the space born sensor for the same surface reflectance and AOTs could be explained solely by the change in aerosol layer height, provided that the sun-photometer derived Angstrom exponent is approximately constant for all the AOT measurements. In order to check the possibility of any systematic change in the size distribution of aerosol, preliminary analysis has been carried out using ground based sun photometer data. Temporal profiles

of the Angstrom exponent ( $\alpha$ ), derived by fitting AOT in wavelength, are shown in Fig. 3. The  $\alpha$ -Values are clumped into three groups based on the three models for 412 and 443 nm. It is found that angstrom exponent decreases in general from Dec. to May (fig.3).

The mean and the standard deviation (denoted by vertical error bars for each group) are shown in the fig. 3. Though the spread is large the averages show  $\alpha$ -values decreasing in time. Higher value of  $\alpha$  is an indicator of dominance of fine-mode particles with associated higher spectral variation in AOT by Dey et al. [13]. Decrease in angstrom exponent corresponds to the increase in coarse mode particles. As discussed earlier because of increase in temperature soil becomes drier and more dust is thrown into the atmosphere due to advection. These results in the increased dust content i.e. increased coarse mode particles content in the atmosphere and therefore modify the size distribution resulting in decrease in the angstrom exponent values from Dec. to May. Since the method uses molecular scattering background for the retrieval of aerosol absorption properties, retrievals are sensitive to aerosol layer height.

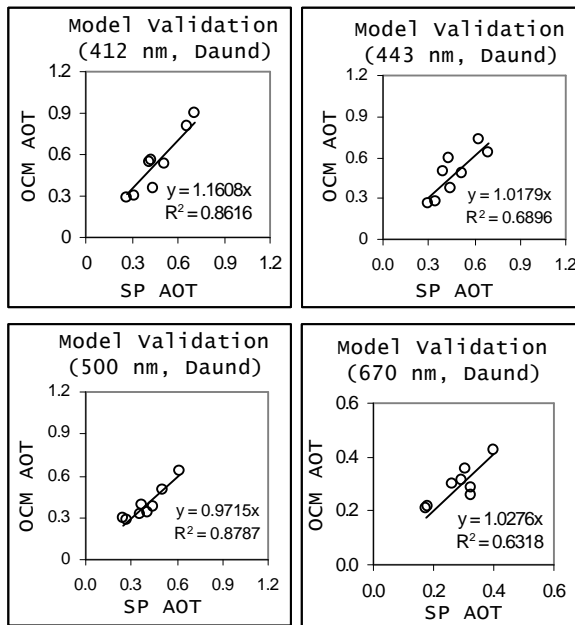


**Fig. 2: Comparison of OCM derived AOTs with the AOTs measured by sun-photometer at corresponding wavelengths on a one to one scale.**

Aerosol effect is most dominant in the visible and near IR part of the solar spectrum. Also in visible and near IR region a very small part of the total TOA radiance is contributed by the aerosol scattering except for the TOA measured over dark targets like water body or vegetation. Most of the satellite-based studies, including the one presented here, therefore use the dark target approach for the characterization of aerosol over land. In the near UV the atmospheric signal is much larger than its counterpart in visible region. Taking advantage of this fact absorbing aerosol index is defined to characterize aerosol using Earth Probe-Total Ozone Mapping Spectrometer [EP-TOMS] data.

In near UV region backscattered radiation mostly consists of molecular scattering, which can be safely assumed to be constant, therefore any change in the amount of backscattered radiation can be attributed to the change in aerosol absorption. On the basis of a relationship between the

ratio of backscattered radiance at 340 nm and 380 nm ratio and the 380-nm back-scattered radiance measured by EP-TOMS, a direct way of determining aerosol properties taking advantage of the spectral contrast change with respect to molecular atmosphere is reported by Torres et al. 1998 [6]. At wavelengths longer than 320 nm, where ozone absorption is weak, effect of absorbing aerosol on transmitted radiation becomes important. The spectral dependence of the change in scattered radiance is proportional to aerosol scattering, while the magnitude of this change is proportional to aerosol absorption. Torres et al. also suggested an alternate method based on the 340/380 TOA radiance ratios for aerosol type discrimination. The TOA radiance ratio 340/380 vs. 380 nm radiance plot can be used to clearly separate the aerosol types and/or aerosol models. The slopes of the lines can be related to the SSA, which in turn to aerosol models. They also showed that this alternate method is valid for wavelengths up to 450 nm on x-axis. This method is not very sensitive to the height of the aerosol layer. In the present study, the same methodology is applied to the forward-scattered radiation measured by the sun photometer in 340 and 440 nm channels. Firstly, the sun photometric radiance data is arranged into three groups as per the three aerosol models at 412 and 443 nm wavelengths, and then the radiance ratio at 340 and 440 nm wavelengths is plotted against the radiance at 440 nm (Fig. 4). We find three distinct relationships for the three groups of data, indicating change in aerosol absorption properties from Dec. to May. It should be noted here that the distinction is made on the basis of total incoming columnar radiance measured by the sun photometer at ground level; change in aerosol height is not a affecting parameter. This study manifests the seasonal behavior of aerosols over the study area qualitatively. The lines shown in the fig. 4 could be used further to compute SSA for the study area. These results reinforce our observation that the changing aerosol types and models are responsible for giving rise to three models of AOT retrievals.

The OCM based AOT maps generated for the region centered at Pune at all the four wavelengths show low AOT values along the western Sahyadri mountain ranges, which is sparsely populated. The pristine environment of the mountain range elucidates the reason behind the low aerosol loading resulting in the low AOTs as compared to the rest of the mapped area are seen in the northwest of Pune. In this region presence of the fine mode pollutant particles are expected to dominate the total aerosol content in the atmosphere due to urban sprawl and industrial growth along Pune-Mumbai highway. These industries are potential source of fine mode pollutant particles. Higher AOTs at lower wavelengths on the map is a signature of presence of fine mode pollutant particles in this region originated from the nearby industrial area.

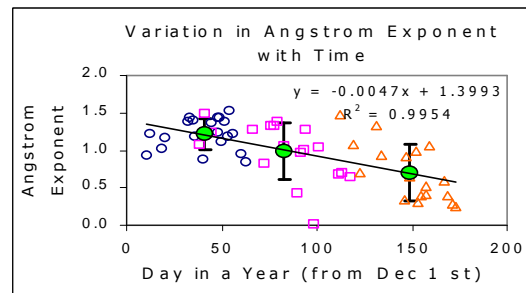


**Fig. 3. The temporal profile of AE and it's bimonthly averages.**

On the other hand in the 670 nm AOT map, arid region situated towards the northeast and the east of Pune shows comparatively higher AOT than the other parts of the map due to dry-land agricultural activities.

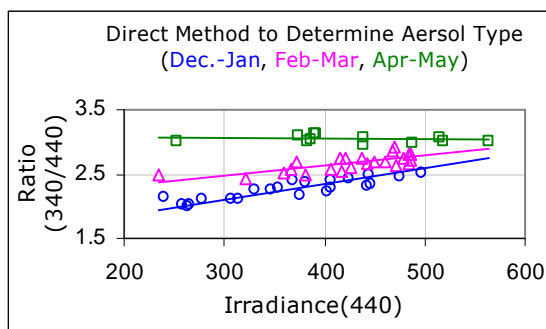


**Fig. 4. The 340/440 ratio vs. 440 nm plot from sun photometer data showing the three major aerosol models for Dec-Jan., Feb-Mar and Apr-May periods.**

This observation is justified by the fact that an arid area, because of the abundance of the coarse mode dust particles, would show higher AOT at larger wavelengths as compared to the other vegetated areas. Model validity is checked by comparing the mapped AOTs with the measured ones at Daund. They are found to be in good agreement (fig.). At 412 nm model overestimates the AOT by 16%.

### Conclusions:

We have tried to show in this paper that within the errors of the AOT measurements using a sun photometer as well as the within the errors of the TOA radiance measurements by IRS-P4 OCM sensor, and within the variations in the reflectance of TVTs, the change in the aerosol type from Dec. to May on bimonthly basis can be inferred. The performance of the AOT retrieval models show that the AOT estimates are within  $\pm 0.2 \cdot \text{AOT}$  like the AOT estimates from MODIS data. Unlike MODIS based methodology, our methodology follows simplified approach for AOT modeling from TVTs radiances.

S. N.	Time Period	Equation to find SSA (y: Ratio(340 /440), x: Irradiance (440))	R <sup>2</sup>
1	Dec.- Jan	$y = 0.0025x + 1.3251$	0.64
2	Feb.- Mar	$y = 0.0015x + 2.0275$	0.51
3	Apr.- May	$y = -0.0001x + 3.0912$	0.03

**Table 3. Relations for the three lines shown in the fig. 4.**

The AOT retrieval models are used to map AOT over 180x180 km<sup>2</sup> areas. The maps are validated using independent data sets. The spatial variation of AOT is as per expectations based on topographical variations, agricultural and urban/industrial activities. The spectral AOT maps are used to generate Angstrom Exponent and turbidity coefficient maps. These maps show anti-correlation which is expected based on near Junge type size distribution followed by the aerosols in this region, which are mostly continental type.

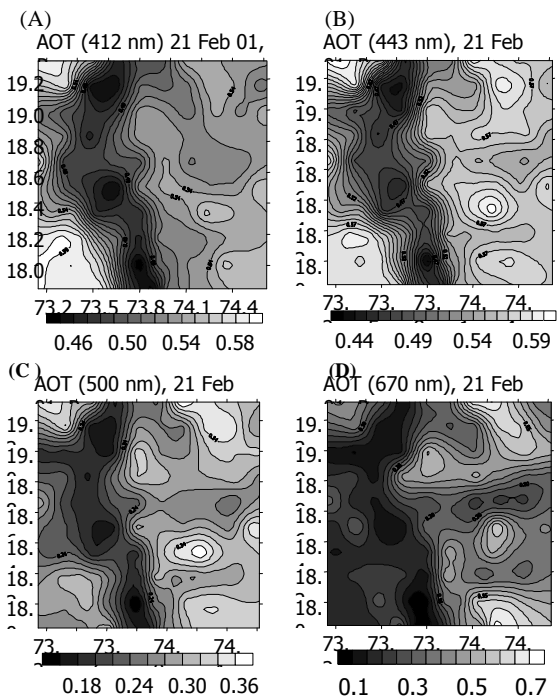


**Fig. 5: AOT maps, centered at Pune at four wavelengths, indicated with each of the figures A, B, C and D. Lower AOTs at four of the wavelengths along the Western Ghat region is clearly seen in each of the maps.**

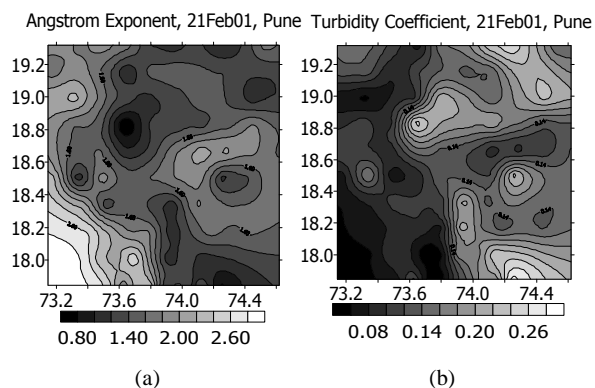


**Fig.6: Maps for two size distribution parameters centered at Pune. Turbidity coefficient map (b) looks like the mirror image of the angstrom exponent map (a). The inverse relationship expected between the two parameters is seen on a spatial map.**

It is shown that the changing AOT retrieval models are reflection of the changing aerosol types exhibited by the changing AE. The sun photometer measured surface level radiance also shows confirm this aspect. It is known that the TOA aerosol radiance depends mainly on the aerosol type and to a certain extent on the height of the aerosol layer. The contributions due to the change in layer height need to be ascertained.

The methodology developed in this work, however, has its own limitations. It is applicable to vegetated areas and can not be applied to areas of snow and desert cover; which are devoid of vegetation. The spatial resolution should be adequate enough to find pixels of NDVI > 0.5. In case of altogether different

surface type, where the contribution from background soil to the surface reflectance is significantly different from that at the model development site, may be due to adjacency effect, it is expected to show large errors in AOT retrievals.

#### Acknowledgment

We are thankful to Project Management Board of the ISRO-GBP Program (Dept. of Space, Govt. of India) for encouragements and financially supporting this work under ISRO-GBP WG-IIA on "Aerosols and Radiative Forcing". We are thankful to Prof. R.Sridharan, Director, SPL/VSSC and Chairman, ISRO-GBP WG-II and Dr. K. Krishanmoorthy, Co-Chairman, ISRO-GBP WG-IIA for critically reviewing this work in WG-II meetings. We are also thankful to Dr. R.R. Navalgund, Director, SAC, Mr. J. S. Parihar, Gr. Director, ARG/SAC, Dr. M. Chackraborty, Head, TSDD/SAC for their constant encouragement.

#### References:

1. Kaufman et al. 2002, A satellite View of Aerosol in the Climate System, vol. 102, pp6831-64
2. Liu C. H. et al. 1996, An Image based Algorithm of Aerosol Characteristics and Surface Reflectance from Satellite Images, *Int. J. Remote Sensing*, vol. 17, No.17, 3477-3500
3. Hoyningen-Huene, W. von et al. 2003, Retrieval of aerosol optical thickness over land surfaces from top-of-atmosphere radiance, *JGR*. Vol.108, No. D9
4. Torres et al. 1998, Derivation of aerosol properties from satellite measurements of backscattered ultraviolet radiation: Theoretical basis, *JGR*, vol. 103, No. D14, 17099-17110
5. Rege Rajshree, M.B. Potdar, P.C.S Devara and B. P. Agrawal, 2005, Proc. ISRO-GBP WG-II meeting, PRL, Ahmedabad.
6. Prospero J.M. et al. 2002, Environmental characterization of global sources of atmospheric soil dust identified with the NIMBUS 7 Total Ozone Mapping Spectrometer (TOMS) absorbing aerosol product. *Review of Geophysics*, vol. 40, no.1, 2-1 – 2-31.
7. Jethva H. et al. 2005, Seasonal variation of aerosol over the Indo-Gangetic basin. *JGR*, vol. 110, D21204.
8. Potdar, M.B. et al., 2004, Remote sensing of spectral signatures of tropospheric aerosols, *Earth and Planetary Sciences, Proc. Indian Academy of Sciences*, Vol. 113, No. 1, pp. 103-116.
9. Hsu, N.C. et al. 1999, Comparison of the TOMS aerosol index with Sun-Photometer aerosol optical thickness: Results and applications, *JGR*, vol. 104, No.D6, 6269-6279.
10. Bergstrom, R. W. et al. Wavelength Dependence of the Absorption of Black Carbon Particles: Predictions and Results from the TARFOX Experiment and Implications for the Aerosol Single Scattering Albedo, *J Atmos Sci*, vol. 59, 567-576.
11. King, M. D. et al. Aerosol Size distributions Obtained by Inversion of Spectral Optical depth Measurements, *J Atmos Sci*, vol. 35, 2153-2167.
12. Thierry Elias et al. 2004, Estimation of the aerosol single scattering albedo at several wavelengths without making assumption on aerosol microphysics, *Optica Pura Y Aplicada* vol 37, num 3.
13. Dey, S., et al., 2004, Influence of dust storms on aerosol optical properties over the Indo-Gangetic basin, *J. Geophys. Res.*, 109, doi: 1029/2004JD004924.
14. Curcio, J.A., 1961, Evaluation of Atmospheric aerosol particle size distribution from scattering measurements in the visible and infrared, *J. opt. Soc. Amer.*, vol. 51, 548 – 551.